

# Co-evolution of network structure and consumer inequality in a spatially explicit model of energetic resource acquisition

Natalie Davis <sup>a,b,\*</sup>, Andrew Jarvis <sup>a</sup>, J. Gareth Polhill <sup>b</sup>

<sup>a</sup> Lancaster Environment Centre, Lancaster University, Lancaster, UK

<sup>b</sup> The James Hutton Institute, Aberdeen, UK

## ARTICLE INFO

### Article history:

Received 1 April 2022

Received in revised form 27 July 2022

Available online 22 October 2022

### Keywords:

Resource network development

Resource inequality

Environmental heterogeneity

Flow consistent

Social–ecological systems

Agent-based model

## ABSTRACT

Energetic resources in ecological and social–ecological systems are distributed through complex networks, which co-evolve with the system and consumers to move resources from points of origin to those of end use. Past research has focused on effects of spatiotemporal resource heterogeneity in ecosystems and society, or socioeconomic drivers of inequality, with less attention to interactions between resource network structure and population-level outcomes. Here, we develop a spatially explicit, stock-flow consistent agent-based model of generic consumers building and crossing links between resources, and we explore the co-evolution of the emergent network structure and inequality in consumers' resource reserves across three distinct landscapes. We show that the consumer inequality initially decreased during network expansion, then increased rapidly as the network reached a more stable state. The spatial distribution of resources in each of the three landscapes constrained the structures that could emerge, and therefore the specific rates and timings of these dynamics. This work demonstrates the use of energetically consistent modelling to understand possible relationships among a spatially distributed set of resources, the network structure that connects them to a population, and inequality in that population. This can provide a theoretical underpinning informing further work to better understand causes of resource inequality and heterogeneity in observed systems.

© 2022 The Authors. Published by Elsevier B.V. This is an open access article under the CC BY license (<http://creativecommons.org/licenses/by/4.0/>).

## 1. Introduction

Given the universal requirement of energy for maintenance, growth, and development, much of the dynamics of biological, ecological, and social systems are driven by the procurement and relocation of energetic resources from points of acquisition to points of consumption and end use. The infrastructure enabling this relocation can be conceptualised as a series of nested, interconnected resource acquisition, distribution, and end-use networks ('RADE' networks, e.g. [1]). Examples of RADE networks include vascular systems, freight transport and distribution networks, foraging trails, electricity grids, and soil macropore networks. The complex structures and dynamics of these networks, and the systems relying on them, arise from the interactions of the many heterogeneous actors shaping the network, whose states are intrinsically connected to the resource flows they can access via the network. Therefore, a bottom-up approach to representing and analysing these networks is useful to explore their development, and the interacting evolution of the network and those relying on it. This work presents a simple but fully energetically and physically consistent agent-based

\* Correspondence to: Copernicus Institute of Sustainable Development, Utrecht University, Utrecht, The Netherlands.  
E-mail address: [ndavis.research@gmail.com](mailto:ndavis.research@gmail.com) (N. Davis).

model (ABM) of RADE network development and uses it to explore the question *how does inequality in resource reserves co-evolve with the structure of the network that is built by and provides access to these resources?*

The dynamics of resource distribution through RADE networks are constrained by the same physical and thermodynamic laws that govern all physical substances on Earth. Specifically, the conservation of energy and matter entails that the total energetic output of the networks must be equal to the inputs. In all systems, energy transformations also consume energy, which is released from the system as entropy, often in the form of heat. The proportion of potential energy available to the end consumers to do useful work is therefore less than the original energetic inputs to a network. These transformations can take the form of state changes of the resource itself, such as through processing. More relevant to the work here, however, is the friction experienced when moving matter through space and the resulting transformation of some energy into heat, underscoring the importance of spatial dimension in tracing the energy use of a system. When stored energy is considered, the full energy balance may have to be resolved over multiple timescales, but the reduction in free energy due to frictional losses still applies.

After the energy consumption in moving the resources and maintaining both the network and the consumers is considered, the net excess resource flow can be used for growth and development of the system and its constituents. This can take the form of expansion and improvement of the RADE network itself, such as increasing the efficiency of future resource flows to minimise frictional losses incurred during transport. However, any initial heterogeneity in the spatial distribution of resources or configuration of the network can lead to unequal resource access for consumers, who would then have different net energy reserves to reinvest in developing the network.

These individual differences in energy consumption are a key driver of the dynamics in ecological and social-ecological systems. Discussions of inter-species heterogeneity often focus on the environmental and ecological conditions governing the spatiotemporal distribution of resources, as the quantities, types, and accessibility of resources determine the amount and complexity of life that an area can support. When the heterogeneity in resource availability occurs at biologically relevant scales to the species present, it can enhance biodiversity and ecosystem stability [2], leading to a reported positive resource ‘heterogeneity–biodiversity’ relationship (see reviews in Tews et al. [3], Stein et al. [4]). When the resource heterogeneity is due to anthropogenic modification or fragmentation, however, it can isolate species and individuals in unsuitable habitat patches, making populations vulnerable to stochastic extinctions [3,5,6].

In contrast, ‘inequality’ is usually discussed in terms of intra-species differences – usually between humans – in the quality or quantity of resources they can access to meet their basic needs, and any excess [7]. This has typically been studied through an economic or sociological lens [e.g. 8,9]. While financial inequality undoubtedly affects the distribution of physical, energetic resources in society such as food and fuel, insecurity in these resources has also been implicated in increasing economic inequality and limiting the prospects of individuals to lift themselves out of poverty [10–13], and negatively impacting health [14,15] and environmental sustainability [16]. Given these considerable impacts of resource heterogeneity in both ecosystems and social-ecological systems, it is crucial to understand the emergence of heterogeneity and inequality to guide efforts in management and alleviation.

One method that has shown considerable promise in both understanding the emergence of complex phenomena such as network structure or resource inequality, and enabling spatially explicit system representations, is agent-based modelling. In ABMs, the system-level phenomena emerge from the decentralised decisions and interactions of autonomous agents. This can be used to explore feedbacks and other complex causal structures arising from simple behavioural rules and interactions, without requiring the structure of feedbacks or other system-level dynamics to be specified in advance. For example, Dragulescu and Yakovenko [17] show that inequality, in the form of a power law distribution of wealth, can emerge through random wealth exchange between agents. Other resource-based models have focused on the energy grid [18,19], trade in the food system [20–22], foraging [23–27], and inequality in consumption among consumers searching a landscape [28,29]. Additionally, models utilising fixed agents and network structures have highlighted the how the combination of social dynamics and resource heterogeneity [30] and resource diffusion [31] can drive sustainable patterns of consumption or system collapse. However, none focus on linking heterogeneity in consumer resource reserves to the spatial evolution of resource networks that they create and use, thereby growing these networks in an energetically-consistent framework.

The work presented here develops and analyses a spatially explicit and energetically consistent theoretical ABM of resource acquisition. The network structure emerges over time from consumers building and maintaining links to maximise their resource consumption, within their currently available resource capacity. The model is then used to explore a stylised case study of the co-evolution of RADE network structure and inequality in resource reserves, and how this is constrained by landscape heterogeneity.

## 2. Model description

To explore the co-evolutionary relationship between network structure and energetic resource inequality in a population, a model should incorporate the thermodynamic laws constraining transformations of matter and energy in earth systems, introduced above, to ensure that any emergent dynamics observed are physically and energetically consistent. In the context of RADE network models, energetic and physical consistency entails that only net energy flows can be re-invested in maintaining or expanding the network or securing future resources. The network structure and inequality that emerges then reflects this constraint. In this way, energetic consistency links the two emergent aspects of inequality

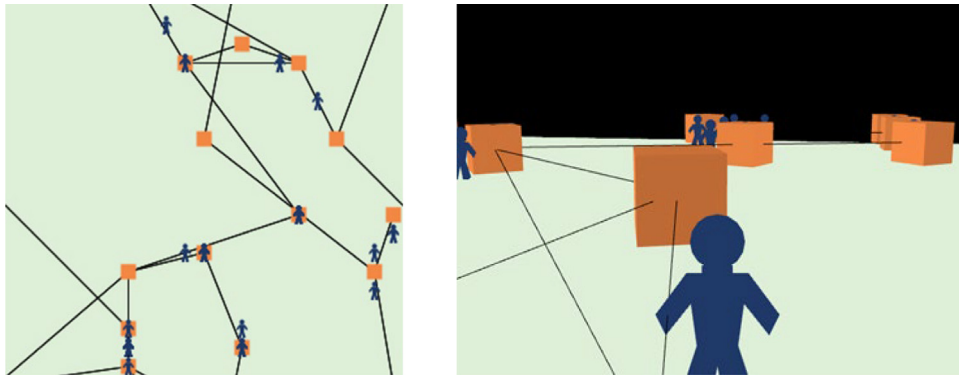


**Fig. 1. Images from the simulations.** The blue figures represent the consumers, the orange boxes represent resources, and the black lines show which patches have been transformed into links.

in resource reserves and network structure, such that the network that emerges is physically possible, and any persistent inequality is related to the structure of the network that was built based on – and continues to facilitate – potentially differential access to resources. Without explicit consideration of energy balances, the network structure and state of individuals operating within it will not necessarily reflect physically possible processes of energy investment.

In the model presented here, the equations governing agent decisions and describing model dynamics were based on the stock-flow consistent equations of systems dynamics models, ensuring that units were balanced, and the model maintained physical and energetic consistency as far as possible. This model extends beyond typical stock-flow consistent analyses, however, by comparing resource consumption across a population, and analysing the interactions between the inequality of consumption and the emergent network structure. By focusing on the first principles of energy conservation and transformation, a realistic network structure and level of persistent inequality are allowed to emerge, rather than assuming these as fixed. In the remainder of this section, the characteristics of the agents, sequence of events, and equations defining agent behavioural rules and model dynamics will be discussed. A full model description following the Overview, Design Concepts, and Details (ODD) protocol is in Appendix 1, and the model code is available on Modelling Commons ('Network Development ABM') and Zenodo [32].

The model consists of agents, called consumers, who build and use links to navigate across their environment between resources (Fig. 1). The environment is represented as a collection of patches, with each patch having a baseline roughness. The links are then series of patches along the shortest path between resources. The consumers store and use energy from the resources to meet their basal metabolic requirements, and to build and repair more links, by investing net energy to decrease patches' roughness and make them crossable. The use of patches incorporates environmental heterogeneity, such that energy investment in links is proportional to both the length of the link and the innate irregularity of the environment. The consumers' aim is to maximise their individual energy consumption to allow for reproduction and future network expansion and improvement. To do so, they use a simple discounting model to choose between resources within their vicinity, calculating the expected time-discounted energetic costs and returns for each, and choosing the resource with the maximum return (if more than one option has the same maximum estimated return, a random selection is made among them).

At the start of each timestep, each consumer attempts to consume its basal metabolic requirement from its energy reserves. If the consumer does not have adequate energy to cover this, it dies. Otherwise, the consumer updates its vision radius, which determines the boundaries of the area centred on the consumer's current location that it can scan for resources. The vision radius is calculated as

$$V_i = \frac{E_{R_i}}{P_i}, \quad (1)$$

where  $V_i$ ,  $P_i$ , and  $E_{R_i}$  are the vision radius, risk penchant, and accumulated energy reserves of consumer  $i$ , respectively. The risk penchant is a constant (in units<sup>1</sup> of energy per unit length, or  $\text{J m}^{-1}$ ) that determines how much energy the consumer is willing to risk, or invest, on building, repairing, or walking along links.

After this, consumers who are not currently building or walking assess the resources within their vision radius. Based on their expected consumption from the resource they are located on, and the expected provision of the resources they can evaluate, they decide whether to stay where they are, or move to a different resource by building a new link, repairing an existing link, or walking across an existing link. Consumers who are building or repairing links walk across them simultaneously.

<sup>1</sup> Base SI units are used for the variables and equations here for generalisability, not to represent values for any specific observable system.

The consumers use a simple discounting model to choose between resources, which places a higher weight on near-term returns. Consumers evaluate each resource in their vision radius, including their current location, by applying a discounting function with their rate of time preference  $\rho$  to the expected consumption gain  $E_G$  at each timestep  $t$  of their overall time horizon  $T$ . The expected consumption gain is zero over the timesteps that they are moving toward the resource, and after they arrive, is determined by the resource's capacity and consumer's consumption rate (described below). From this, they subtract the expected costs  $C$  of each timestep, calculated as the energy required to cross each intermediary patch, including any path construction, discussed below. The sum of the differences is the net discounted utility,  $U$ . The consumer then chooses the action with the maximum  $U$ .

$$\max U = \max \sum_{t=0}^{T-1} \frac{(E_{G_t}^{1-\rho} - 1)(1 + \rho^{-t})}{1 - \rho} - C_t. \quad (2)$$

Time preferences and discounting have been demonstrated across a range of species [see reviews in Hannon [33], Vanderveldt et al. [34]] and are included in most microeconomic models since their introduction by Ramsey [35]. By discounting returns in the future, which are more uncertain given the possibility of other consumers simultaneously constructing links or consuming resources, each consumer attempts to minimise risk and maximise energy consumption, within the limits of the energy it can invest.

If a consumer calculates that staying on their current resource is the optimal choice according to Eq. (2), they remain there. Any such consumers who are not currently building, repairing, or walking links, and have at least twice their initial energy allocation, produce an offspring. The offspring inherits all traits from its parent, such as risk penchant, time preference, and basal metabolism. Moreover, offspring are also given the same initial energy reserves as their parent, with the parent transferring this amount from their own energy reserves when they reproduce. This ensures consistency of the overall energy balance of the model. Reproduction was included to reflect observed ecological and social-ecological systems where population size evolves alongside the network structure and inequality, which can allow the system to explore a range of possible states.

Consumers who are building, repairing, or walking continue to do so, moving one patch per timestep along the patches closest to the shortest path between the consumers' initial and target resources. As the current level of roughness of each patch determines the energy required to cross it, consumers use the heuristic of reducing the roughness to a minimum, or increasing the smoothness to its maximum, such that they spend less energy to then cross the patch.

Specifically, the current roughness of each patch  $\theta$ ,  $R_\theta$  (in N), is inversely proportional to the current level of work done to smooth it into a link ( $L_\theta$ , in J),

$$R_\theta = \frac{\beta_\theta}{L_\theta}, \quad (3)$$

where  $\beta_\theta$  is a conversion factor equal to the baseline roughness of the patch, with units of N J, and  $L_\theta$  is bounded from below at 1. The links can be conceptualised as stocks of infrastructure, or work that has been embodied into the landscape. The rate of change of this infrastructure/work at each timestep is

$$\frac{\Delta dL_\theta}{\Delta dt} = E_{B_\theta} - kL_\theta, \quad (4)$$

where  $E_{B_\theta}$  is the energy invested by a consumer in patch  $\theta$ , and  $k$  is the rate of decay, such that the decay of a link-patch at each timestep is a first-order decay process, proportional to the current level of infrastructure.

As introduced, the energy spent at a given timestep to build or repair that patch, leading to the accumulation of this embodied energy  $L$ , decreases the roughness of the patch. In these simulations, this is simplified as

$$E_{B_\theta} = S (R_\theta - R_{min}), \quad (5)$$

or the energy required to decrease the patch's roughness to the minimum. Here,  $S$  (in  $m s^{-1}$ ) represents the rate of work – one patch per timestep – to build the link. For simplicity, we bound  $R_\theta$  from below at 1, which bounds  $L_\theta$  from above at  $\beta_\theta$  when  $L_\theta$  is at its maximum due to energy investment (see Eq. (3)). The energy required to cross the patch, assuming the same constant speed for walking and building of  $S =$  one patch per timestep, is

$$E_{W_\theta} = SR_\theta. \quad (6)$$

At the end of each timestep, any consumers who are already located on resources or have reached their intended destination consume as much resource as they can, up to the lesser of their maximum consumption rate (determined by a model parameter), or the total supply of that resource. If there are more consumers on a resource than it can support, the consumers split the available resource supply evenly. In this way, there is competition for resources, but it is indirect rather than more overt territoriality. Resources that are below their maximum capacity also regrow linearly at a fixed rate per timestep. While this introduces new energy into the system, it is assumed that the boundaries of the 'world' inhabited by the consumers includes processes such as nutrient cycling and rainfall that govern resource regrowth, which are parameterised rather than modelled explicitly for simplicity. Moreover, the consumer states and the network structure that they create and use, as the focus of the work here, are still energetically consistent.

Due to computational restrictions, consumers cannot make their decisions or act simultaneously. Instead, they act in a random order each timestep, necessarily impacting one another indirectly through building and maintaining links. Resource consumption occurs for all consumers located on a resource simultaneously, but consumers who act at the end of a given timestep may benefit from earlier energy investments. This stochasticity can introduce inequality before any construction or energy consumption, and regardless of the spatiotemporal heterogeneity of the resources. While unavoidable in the context of the model here, it is also not necessarily unrealistic, as consumers of all species experience interference and indirect interaction of their contemporaries. However, this can complicate understanding of how inequality emerges in such networks, which will be revisited in Section 5.

The final energy balance of a consumer includes energy gained from consumption ( $E_G$ ) minus energy spent on building or repairing links ( $E_B$ ), walking links ( $E_W$ ), individual maintenance (basal metabolism  $E_M$ ), and any energy passed on to offspring ( $E_O$ ). The balance of these terms over time,  $E_R$  (from Eq. (1)), forms the energy reserves that are used for future metabolism and reproduction, and determine how much energy the consumer can reinvest in expanding and maintaining the network:

$$\frac{\Delta dE_R}{\Delta dt} = E_G - E_B - E_W - E_M - E_O. \quad (7)$$

Although the resources in the model regrow each timestep, and consumers are not territorial over their occupied resources or built links, there is clearly a component to the model that creates the possibility for competition and inequality. Consumers consume resources that others were targeting, and they move through spaces with varying degrees of patch roughness, existing architecture, and resource availability. While consumers follow the same rules for making choices, their individual rates of time preference and horizon, risk penchant, energy reserves, and location mean that they follow divergent life histories, further separated by their asynchronous decisions and actions, discussed above. When enacted over the landscape, this can give rise to the interconnected inequality and network structure that will be explored.

### 3. Methods

#### 3.1. Generating the landscape

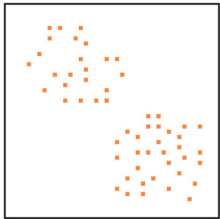
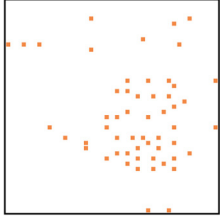
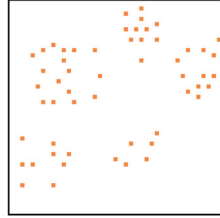
The landscape of the model was represented by a grid of patches on a toroid with an inherent or baseline ‘roughness’ (Eqs. (3)–(6)). The model also required a map of resource node locations. The full description of landscape generation, and the patch and resource landscapes tested in the sensitivity analysis and model exploration, are included in Appendices 1 and 2, and only the landscapes used in the final experiments are listed in Table 1. For the experiments explored in the remainder of the text, only ‘random’ patches were used: patches had uniformly random baseline roughness within a specified range, with the baseline roughness fixed for each patch across all runs.

The landscapes for the final experiments were chosen to represent three distinct combinations of denser clumps with shorter intra-group distances, and longer inter-group distances. These are not meant to allow an exhaustive analysis of the link between resource spatial distribution and system outcomes, but to illustrate landscapes of resources with potentially different effects on the network structure and population state that evolve across them. While the names ‘Cities’, ‘Villages’ and ‘Transition’ were used to reflect how resources might be distributed in human settlements, comparable distributions could be easily identified in a range of ecosystems.

#### 3.2. Experiments

Before the final experiments were run, a sensitivity analysis was performed (details in Appendix 1), including a full model exploration using a  $2^K$  factorial approach [36] (Appendix 2). The sensitivity analysis first compared distributions of outcome variables at differing run lengths (in timesteps) and number of replicates for high, medium, and low input parameter levels, and a range of possible landscape types. The model exploration then tested every possible combination of high and low values for input parameters, across each of the final resource maps (Table 1) and two additional patch maps. In summary, the model exploration showed that the size of the landscape did not qualitatively affect the outcomes, but that link decay rate, mean resource capacity, population size, and maximum baseline patch roughness parameters all affected network and population outcomes. Specifically, higher inequality in consumer resource reserves was linked to lower mean resource capacity and higher initial population sizes, as either or both conditions increased competition for resources. The total link length of the network was higher in runs with lower link decay rate, lower baseline patch roughness, higher population size, higher mean resource capacity, or a combination thereof, as these conditions decreased the cost and increased the available resources and labour to construct and maintain a larger network. While insightful in clarifying model dynamics, the high number of runs required for the model exploration did not allow for the in-depth analysis of network and consumer inequality co-evolution, and several parameterisations led to a lack of network construction and maintenance, or population collapse (Appendix 2). While these are interesting phenomena to explore in future work, the focus here is on the emergence and persistence of resource inequality and its co-evolution with network structure, rather than population or network collapse. Therefore, only a subset of the runs, using a parameterisation which resulted in consistent network construction and relative population stability, is presented here for clarity. Final values for each parameter of the runs presented in the main text, hereon called the final experiments, are given in Table 2.

**Table 1**  
Descriptions and diagrams of resource maps used in final experiments.

Resource map name	Description	Illustration
Cities	Resources are grouped into two larger 'cities'. Mean (standard deviation, SD) of distance between resources: 2.81 (0.60) Min. distance: 2 Max. distance: 3.61	
Transition	Resources are grouped into one larger 'city' with some spread outward into the surrounding area. Mean (SD) of distance between resources: 3.88 (2.09) Min. distance: 1 Max. distance: 7.21	
Villages	Resources are grouped into 5 smaller 'villages'. Mean (SD) of distance between resources: 3.42 (1.03) Min. distance: 2 Max. distance: 5	

The resources are shown in the illustrations as orange squares.

**Table 2**  
The values for each parameter in the final experiments.

Parameter	Value
Number of consumers	500
Maximum baseline patch roughness	6 N
Minimum baseline patch roughness	2 N
Link decay rate ( $k$ )	0.1 J timestep <sup>-1</sup>
Mean resource capacity	45 J
Standard deviation (SD) of resource capacity	2 J
Mean resource regrowth rate	9 J timestep <sup>-1</sup>
SD of resource regrowth rate	1 J timestep <sup>-1</sup>
Mean time horizon ( $T$ )	18 timesteps
SD of time horizon ( $T$ )	4 timesteps
Mean initial energy reserves	70 J
SD of initial energy reserves	15 J
Mean basal metabolism ( $E_M$ )	3 J timestep <sup>-1</sup>
SD of basal metabolism ( $E_M$ )	0.5 J timestep <sup>-1</sup>
Mean consumption rate	5 J timestep <sup>-1</sup>
SD of consumption rate	1 J timestep <sup>-1</sup>
Mean $\rho$	1 timestep <sup>-1</sup>
SD of $\rho$	0.025 timestep <sup>-1</sup>
Mean risk penchant ( $P$ )	72%
SD of risk penchant ( $P$ )	4%

Symbols in brackets refer to equations in Section 2.

### 3.3. Analysis

After each run, simulation-level output variables were calculated using the consumer state variables and the currently constructed links. These covered a range of consumer population metrics, such as the population size and standard



deviation (SD) of consumers' energy reserves, which is used as the measure of inequality, as well as metrics for network size and connectivity. The high-level variables and analyses chosen here were used to reflect the population-level statistics typically applied to measure heterogeneity or inequality in social-ecological systems. They also allowed for quantification of the large, complex networks that emerged, from both link- and node-level perspectives, to compare with the overall population dynamics. Other metrics of consumer inequality and network structure were calculated in the model exploration, but they were found to be highly correlated with the ones used here (Appendix 2). The reported outcome variables are shown in Table 3.

**Table 3**  
Outcome variables calculated for each simulation run.

Variable name	Description
Population size	The number of consumer agents currently active in the simulation
Mean energy reserves, $J$	The mean of consumer energy reserves
Standard deviation (SD) of energy reserves, $J$	The standard deviation of consumer energy reserves
Number of links	The number of links (bi-directional) in the network
Number of (included) resource nodes	The number of resource nodes included in the network
Total link length, $m$	The total link length around the network
Mean link length, $m$	The mean link length
SD of link length, $m$	The standard deviation of link length
Mean node degree	The mean number of links attached to each included resource node

Relevant units shown after variable names correspond to those used for the equations in Section 2.

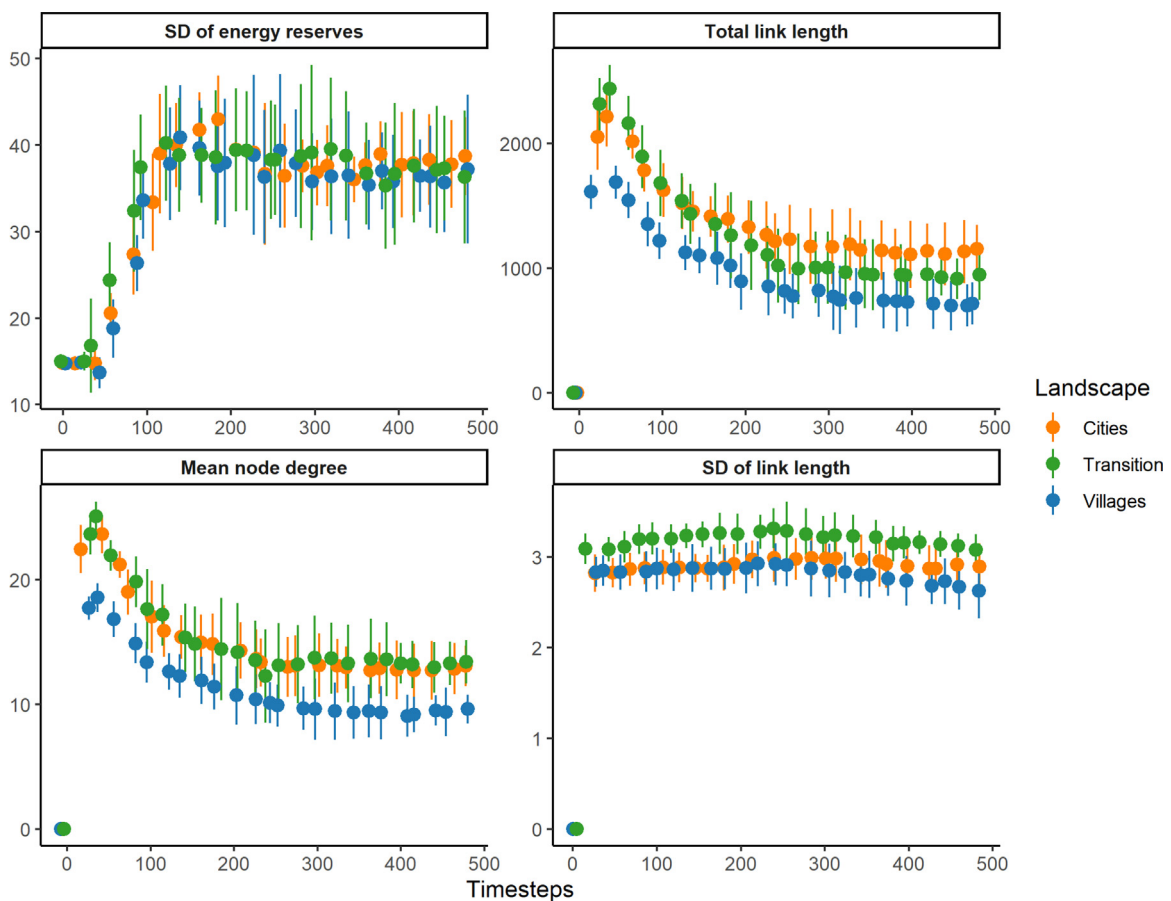


**Fig. 2. Standard deviation (SD) of consumer energy reserves, total link length, mean node degree, and SD of link length over time, for Cities, Transition, and Villages landscapes.** Point and error bars show median and interquartile range (IQR) respectively, over 25 replicates per landscape. Normally distributed noise has been added to the x-value for each point to minimise overplotting and show error bars more clearly. The values at timestep 500 can be taken as indicative of the dynamic equilibrium state for that metric over the remainder of the simulation.

The analytical approach focussed on identifying the inequality and network structure that emerged in each run, and the dynamics of their co-evolution. First, outcome variables were compared visually across landscapes. This captured the role of landscape heterogeneity in the network and consumer outcomes. As simulations can easily generate statistically overpowered samples through replications, conventional frequentist measures were avoided for the preliminary analyses

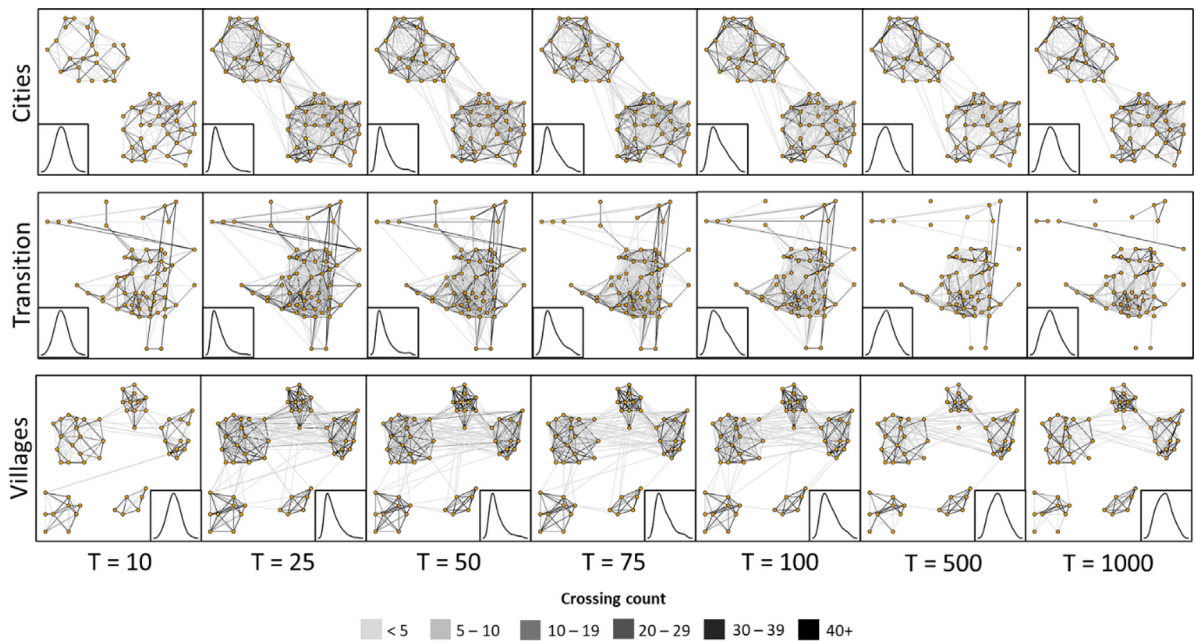


**Fig. 3. The overall network development and consumer energy reserves distributions, for Cities, Transition, and Villages networks, by timestep (T). The lines show the links that were present at each timestep shown, across the 25 replicates per landscape. The line shading represents the total number of times the link was crossed up to that timestep, also across the 25 replicates. The density plot in the inset shows the distribution of consumer energy reserves. As the landscapes were on a torus (see Methods), some of the longer links shown in the Transition and Villages networks wrap around the ‘back’ of the world.**

[37]. The evolution of the networks that emerged in each run was also visualised, by plotting the links that occurred between resources, with line shading indicating the number of times they were crossed. This highlighted the links that were used most frequently, as opposed to those that were built and used only a few times but were maintained through the maintenance of intersecting links. Three networks that showed diverse evolutionary trajectories were then selected from each of the three landscapes, and the evolution of their structures and values of outcome variables were compared, to note any differences that the distinct structural features they displayed had on the measured outcomes (Appendix 3).

Finally, population size, mean and SD of consumer energy reserves, and total link length (as a proxy for total energy investment in the network) were plotted over time together, both with means across all replicates of a given landscape, and individually for each run. This identified major shifts in the dynamics of the simulation, which could be observed from the averaged plots as changes in the slope (breakpoints) of the outcome variables over time. Visual estimates for the breakpoints were quantified for both averaged and individual plots with piecewise regressions, taking the identified slope before each breakpoint as the slope for that segment of the time series. The adjusted  $R^2$  was calculated for each piecewise regression model, and all were found to be over 0.9. The piecewise regression coefficients for the averaged plots of SD of consumer energy reserves and total link length were also compared across landscapes for both landscape alone and landscape/time interactions.

All analyses and visualisations were done in R version 4.0.3 [38], using the igraph [39], segmented [40,41], and ggplot2 libraries [42].

## 4. Results

### 4.1. Network structure and consumer inequality

To answer the question of how network structure and consumer inequality co-evolve in the model, these measures are first explored individually across the landscapes, then in relation to one another. For each of the metrics calculated, all simulations reached their dynamic equilibrium state at around 500 timesteps. While the standard deviation (SD) of energy reserves (inequality) was quite similar across the three landscapes once the simulations had stabilised, it reached its highest point in the Cities networks (Fig. 2). The network metrics were more varied across landscapes, with Transition networks showing the highest peaks for total and SD of link length, and mean node degree.

The overall network development and link use is shown in Fig. 3 (examples of individual networks in each landscape are included in Appendix 3). Across all runs for each landscape, a similar pattern emerges of initially high network density and more uniform use of links, coupled with increasing skewness of energy reserves across the population. This is followed by a pruning phase in which the less frequently crossed links decay away, and both network structure and the distribution of



energy reserves stabilise. This stability is marked by considerably higher consumer inequality than at initialisation (Fig. 2), but the distribution of energy reserves is approximately normal. Additionally, the most used links in the networks (Fig. 3), denoted by darker lines, are often quite short. While longer links do occur, especially during initial construction, shorter links are more frequent across all timesteps and are the ones most used and maintained in later timesteps.

## 4.2. Co-evolution of network structure and inequality

### 4.2.1. Overall dynamics

Fig. 4 shows the overall dynamics of the population size, mean and SD of energy reserves, and total link length, for the Cities landscape. As the general pattern is quite similar across the three landscapes, and individual simulations, this is used as an example to illustrate the general dynamics before comparing specific landscapes and runs.

The major events, labelled on Fig. 4 as 1–4, are as follows:

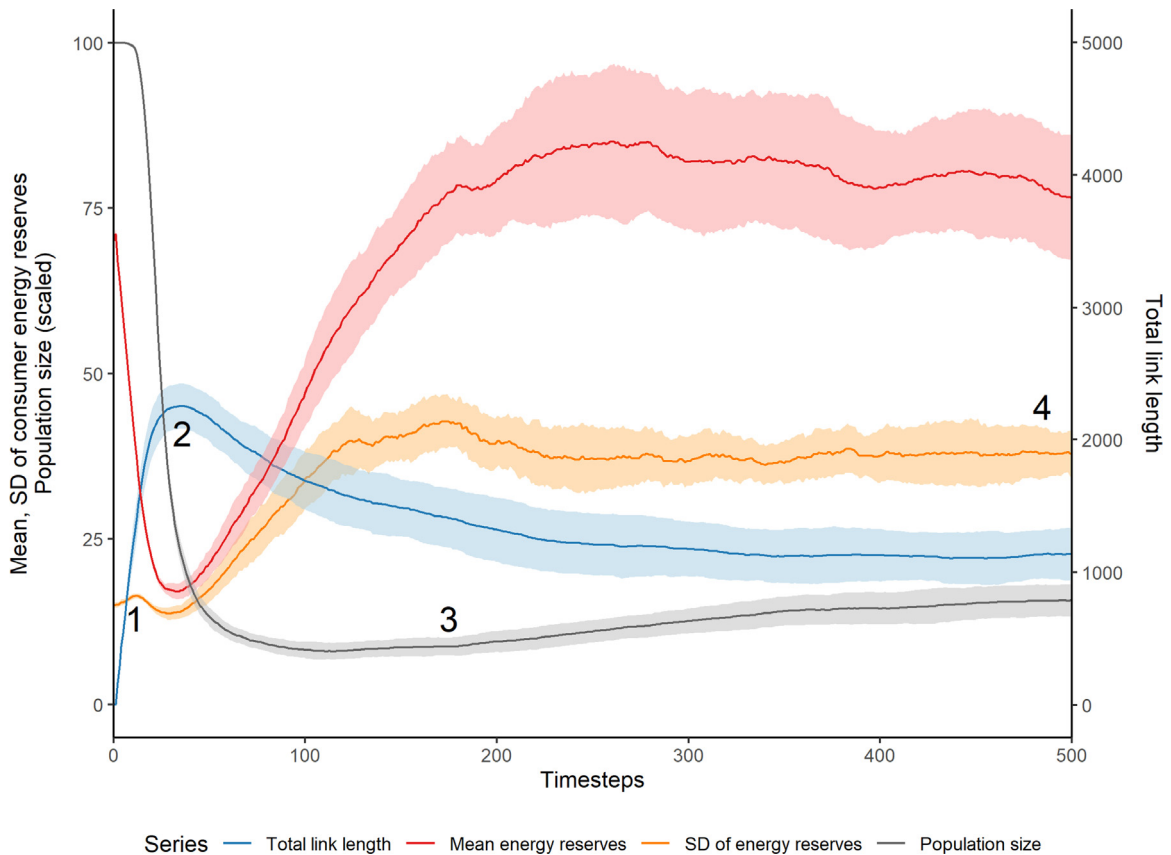


**Fig. 4.** Time series showing evolution of total link length, mean and standard deviation (SD) of consumer energy reserves, and population size for Cities networks, with numeric labels showing main simulation events. The population size is scaled by a factor of 0.2. The lines represent means across 25 replicates, and the shading shows standard deviations. The labelled events are described in the text.

1. Consumers begin constructing links and moving through the network. The total link length increases rapidly with the new links, and the mean energy decreases. As many consumers do not survive the first round of building or are unable to access adequate resources under the initial conditions, the population decreases sharply, as do the mean energy reserves. The SD of consumer energy reserves increases briefly before decreasing slightly.

2. The network reaches its maximum size. The mean and SD of consumer energy reserves are both quite low. Notably, this means that the coefficient of variation of these energy reserves is at its highest; this is a more relative measure of inequality that is reflected in the highly skewed energy reserves distribution between timesteps 25–75 (Fig. 3). Consumer energy reserves, and inequality between them, begin to increase rapidly. Other links that are not maintained start to decay away slowly, giving rise to the more pruned architectures in later timesteps (Fig. 3).

3. After their energy reserves reach the threshold for reproduction, consumers start producing offspring. The population increases in size again, and mean energy reserves and inequality stabilise.

4. The network size and consumer inequality reach a stable equilibrium, without qualitative changes to the network structure or distribution of energy reserves (Figs. 3, A8, A9). Almost all remaining links are frequently used and maintained,

as consumers go back and forth between nodes that provide the optimal balance of resource capacity and proximity to other resources. While consumers cannot plan multiple trips in advance, the resulting network structure shows that links are well-maintained between denser resource patches as consumers frequently commute between these nodes (Figs. 3, A8).

#### 4.2.2. Comparison across landscapes

The overall dynamics illustrated in Fig. 4 are shown for each landscape in Fig. 5. Given the distinctions between the three landscapes, the overall dynamics and timing of network and population phases are quite similar, suggesting that the consumer characteristics and decision-making are dominant in determining the dynamics. However, the differences in the rates of those dynamics and timings of shifts shows the role of the landscape in mediating consumer and resource interactions through the possible network architectures.

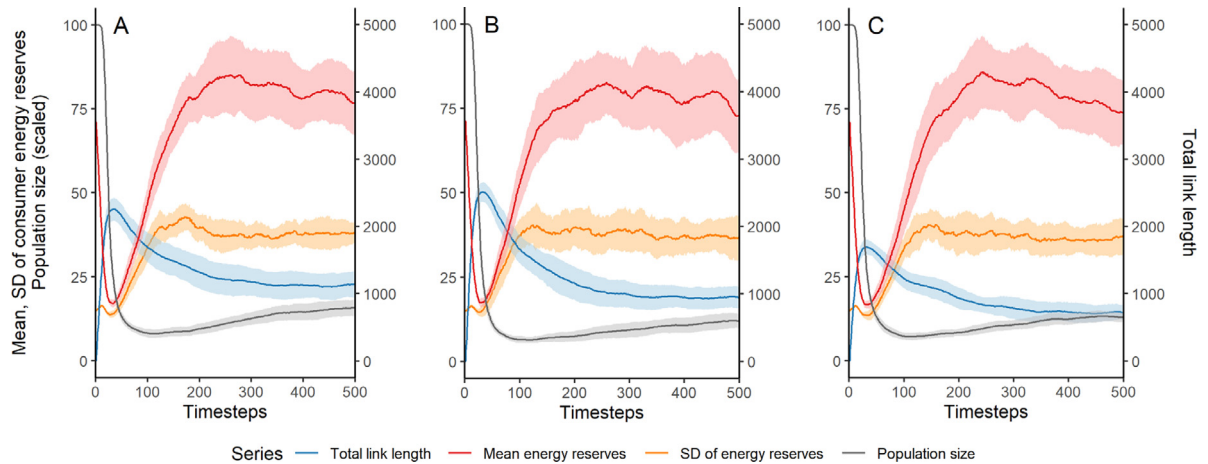


**Fig. 5.** Time series showing evolution of total link length, mean and standard deviation (SD) of consumer energy reserves, and population size for (a) Cities, (b) Transition, and (c) Villages networks. The population size is scaled by a factor of 0.2. The lines represent means across 25 replicates, and the shading shows standard deviations. See Figure A9 for plots showing all 3000 timesteps recorded.

The Cities networks show the highest peak in SD of consumer energy reserves, between timesteps 100–200 (Fig. 5), and a larger decrease after the initial peak, while the SD of consumer energy reserves in Transition and Villages networks quickly stabilise. While the Cities and Transition networks have similar final total link lengths (higher than Villages), the Transition network total link length has a higher peak during its initial construction phase. This is concurrent with the presence of longer ‘city-to-rural’ links in the network maps (Fig. 3).

The breakpoints and slopes for the total link length and SD of energy reserves in the grouped time series plots (Fig. 5), identified by the piecewise regression, are shown in Table 4. These were close to the mean breakpoint and slope for the regressions calculated over the individual runs (Appendix 4).

**Table 4**

The breakpoints and slopes identified by piecewise regression, showing the time points of major state changes in the simulations, and the rate of change of measured variables before and after these changes.

SD of energy reserves							
Landscape	Slope 1 (SE)	Breakpoint 1	Slope 2 (SE)	Breakpoint 2	Slope 3 (SE)	Breakpoint 3	Final slope (SE)
Cities	0.14 (0.01)	11.82	−0.21 (0.01)	26.45	0.31 (0.01)	116.25	0.00 (0.00)***
Transition	0.14 (0.01)	11.51	−0.15 (0.01)***	26.70	0.34 (0.00)***	104.69	0.00 (0.00)***
Villages	0.12 (0.01)	12.30	−0.23 (0.01)	25.68	0.31 (0.00)	123.41	0.00 (0.00)***
Total link length							
Landscape	Slope 1 (SE)	Breakpoint 1	Slope 2 (SE)	Breakpoint 2	Slope 3 (SE)	Breakpoint 3	Final slope (SE)
Cities	20.32 (0.98)	28.03	−9.80 (0.00)***	98.49	−0.07 (0.00)***		
Transition	17.34 (1.15)	28.38	−14.31 (0.11)***	98.50	−0.08 (0.00)***		
Villages	12.53 (0.96)***	27.39	−7.70 (0.06)***	100.47	−0.04 (0.00)***		

The estimates for the slopes are accompanied by their standard error (SE). Shown are the breakpoints and slopes for the three landscapes, with the mean of each outcome variable taken over the replicates at each timestep before calculating the breakpoints. The asterisks denote significantly different coefficients in the regression models, with \*  $p < 0.05$ , \*\*  $p < 0.01$ , \*\*\*  $p < 0.001$ . Full piecewise regression models and comparisons are in Appendix 4 (Tables A6 and A7).

The SD of energy reserves showed similar initial increases across the landscapes, with Villages runs increasing slightly slower and having a slightly later breakpoint. However, the Transition runs had a significantly slower decrease in SD of

energy reserves after the first breakpoint than Cities and Villages did, and faster increase after the second. This increase was contemporary with a significantly faster decrease in total link length after the second breakpoint, during the decay of longer 'city-to-rural' links (Fig. 3). Cities runs had the fastest initial total link length increase and earliest first breakpoint, concurrent with a high density of links constructed rapidly (Fig. 3). In contrast, Villages runs had the slowest increase and latest first breakpoint, as the longer inter-village links took longer to emerge (Fig. 3). Cities and Villages were more similar in both the rates of decrease of total link length after the first breakpoint and increase of SD of energy reserves after the second breakpoint.

## 5. Discussion

In the work presented here, we developed an energetically consistent and spatially explicit ABM of consumers building and using a network to access energetic resources. This was applied to explore the question of how network structure and consumer inequality, measured as differences in resource reserves, co-evolved. In the following, that co-evolution is discussed in the general case, then considering the role of landscape heterogeneity.

### 5.1. Co-evolution of network structure and consumer inequality

Across all three landscapes, the network structure and consumer inequality followed a similar pattern of co-evolution (Fig. 5). Initially, consumer inequality increased with total link length, as consumers made different decisions and experienced a range of energetic costs and consumption possibilities while building. After this initial increase in inequality, construction continued, but inequality decreased as consumers with the lowest energy reserves died; this truncated the distribution of energy reserves in the population by removing consumers from the lower tail.

After this, a negative feedback emerges between consumer inequality and network growth, with inequality increasing faster in networks where the total link length decreases faster (Table 4), and more pruning occurring in networks with higher inequality. Specifically, in networks that had a larger decrease in population, such as the Transition networks where there were more isolated resources for consumers to become trapped (Fig. 3), there were fewer consumers to maintain and use the links built during the initial construction phase. Consequently, more links decayed, and more rapidly (Figs. 3, 5; Table 4). The links that were maintained would have allowed some consumers to navigate between resources while consuming less energy: Consumers in well-connected areas or who moved toward these could minimise construction costs by walking across and maintaining existing links, which required less energy than building new links. Similarly, consumers who were in more dense resource patches could spend less energy to move to another resource if their current resource were drained. Less well-positioned consumers would have to spend more energy to rebuild links to denser or better-connected areas, or they became trapped in less energy-rich parts of the network where they could not build up enough reserves to reconnect to the better developed sections. This would be especially likely in more distant and poorly connected subnetworks, as this could create distinct trajectories for sub-populations with different amounts of resources and links available to them, and cause inequality to increase rapidly. This feedback became apparent through the explicit linking of the energy flows and investment between resources, consumers, and network structure, by making energy use proportional to the distance travelled and roughness of the landscape, and by accounting for any previous energy investments into links across that landscape.

The increase in inequality eventually stopped (Figs. 4 and 5), however, as consumers with adequate energy reserves started to reproduce, which limited inequality by preventing consumers from accumulating too much energy: they had to keep investing energy in the network, or in offspring. Given the multiple interactions between population and network outcomes, it is difficult to determine the exact causes of inequality due to different individual trajectories. Even the high-level analyses of the simple model presented here, however, show that the dynamics and feedbacks that emerge between population size, inequality, and network structure are broadly similar across landscapes, but as will be discussed, the density and location of resources in each landscape constrain the possible networks that can emerge, and therefore regulate the extent of and rates at which these dynamics occur. The energetic consistency of the model means that consumers are constrained in their decisions and ability to reproduce by their energy reserves, which are determined by the resources and links available to them. In turn, however, their energy investments shape the network structure for themselves, other consumers, and future generations. While not a focus of the work here, these findings could emphasise the role of innovation or redistribution in reducing inequality. For example, providing infrastructure funded by a proportional 'tax' on consumer energy reserves or intake could increase equity of access to resources, such as by building and maintaining links to otherwise isolated subnetworks.

Two limitations due to model design decisions could affect these results: the single-resource network and the consumers' decision-making tactics. Given that the resources are all the same type, the model cannot show how unequal access to two or more resources could balance or compound each other. However, single-resource models have been used to illustrate emergent population-level outcomes relevant even to complex human societies (e.g. [28]), and here could be conceptualised as a single resource that can be exchanged for food or materials. Moreover, this model acts as a minimal model, results of which should remain relevant for more complex models with similar basic structures [43]. Further work could explore how the findings scale with additional resource types.

Additionally, the consumers constructing and using the network only thought one action ahead at a time: they did not consider the proximity of a resource to other resources or links, or resource regrowth rates apart from their current

resource. Consumers also had little knowledge of or interaction with one another during the simulation, beyond the indirect stigmergy [44,45] of consuming shared resources and modifying shared network architecture, including concurrent construction of links. This limited the number of free parameters and constrained the consumers' knowledge to local levels, both temporally and spatially. This simplifying assumption allowed for clearer understanding of the generalised model dynamics, and the qualitative results around co-evolution of network structure and consumer inequality are still valid. However, this simplification may have also prevented consumers from constructing more complex network architectures, such as branching networks, which could require collaboration or foresight to identify as optimal for networks connecting multiple points in space.

## 5.2. Effect of landscape heterogeneity on network structure and consumer inequality

In the model presented here, landscape heterogeneity referred to the spatial variability of resources in the landscape, both within and across resource patches. In any system, the landscape constrains the network structures that can emerge to connect resources, but the networks themselves are a co-creation of landscape and consumer behaviour. For example, the total and standard deviation (SD) of link length of the networks presented here were quite similar across landscapes (Fig. 2); the main difference in outcomes between the landscapes was instead the rates and times of network structure and population dynamics (Table 4). Given the low SD of resource capacity (see Table 2), most resources provided similar rewards, such that consumers' decisions were more influenced by the distance between themselves and a potential target resource, the presence of an existing link, and the resulting cost of moving to it. This could also be seen in the larger networks in landscapes with lower baseline roughness, lower decay rate, or both, as identified by the sensitivity analysis (Section 3.2, Appendix 1). Therefore, the rate of total link length increase, and the similar mean link lengths in all landscapes, likely resulted from both the consumers' discounting causing them to prefer to build and maintain shorter links, and the density and spatial distribution of resources constraining what was available to them. Notably, the higher prevalence of shorter links, especially in later timesteps as longer links were less frequently used or maintained, could also suggest a trend toward greater efficiency. Further work is planned to explore differences in energy allocation across individual consumers and over time, and how that relates to the feedbacks between network structure, environmental heterogeneity, and inequality explored here.

As with the network metrics, consumer inequality, measured as the SD of energy reserves, was similar across the three landscapes (Figs. 2 and 5), with differences in maximum inequality and rates of change. Some of this inequality can be attributed to the heterogeneous spatial distribution and capacity of the resources that the consumers moved between; as found in the sensitivity analysis (Section 3.2, Appendix 1), lower mean resource capacity led to higher inequality. Even in a theoretical perfectly uniform landscape, however, slight differences between consumer characteristics, such as time preference or willingness to spend energy on movement, could lead to distinct experiences of the same space. As these would cause consumers to have unique decision-making, energy consumption, and interaction trajectories, this 'experienced heterogeneity' could have a similar effect to physical heterogeneity in accelerating consumer inequality. It could also affect the network structure, creating physical heterogeneity for other consumers, thus making it difficult to separate the effects of physical and experienced heterogeneity on consumer inequality over time.

In the model explored here, the random order of consumer decision-making and movement in each timestep meant that consumers also experienced varying degrees of influence from each other's decisions and actions. This suggests that it is not only the spatiotemporal heterogeneity of resources that drives network structural heterogeneity and consumer inequality, but rather a combination of environmental heterogeneity, differences among consumers and among resources (however minor), and the level of interaction and interference consumers experience, which propagate through the network architecture to create markedly different outcomes for individual consumers. In future work, more exploration of the role of consumer heterogeneity, in both initial attributes and overall decision-making strategies, would help elucidate how this interacts with environmental and network heterogeneity to increase or maintain resource inequality.

## 6. Conclusions

In the work presented here, a spatially explicit and energetically consistent model of resource acquisition was presented. The resource network size, inequality in consumer resource reserves, and their co-evolution were analysed over time and compared across three distinct landscapes. Overall, the results showed broadly similar dynamics and outcomes across the landscapes, but the arrangement of resources constrained the networks that could emerge, and therefore determined the rate at which inequality increased and the network size decreased during pruning of less-used links. Inequality increased during the initial construction phase of the simulation, and again as the network was maintained by and for consumers with enough energy reserves to be able to continue repairing and using links. As it stabilised, the network structure acted to 'fix' the level of inequality in the population, by allowing consumers in more densely linked areas to move between resources without needing to rebuild links, while other consumers had to spend more energy, if they could, building links to access these areas.

While stylised and theoretical in its current state, the model demonstrates the possibility and importance of energetic consistency in understanding resource dynamics. Specifically, it shows how models can incorporate explicit energy balances for both agents and infrastructure, and therefore link the emergent states of each to show how they co-evolve

in a physically possible manner. The findings here illustrate a clear link between the construction and maintenance of a resource network, and the inequality between those constructing and relying on it, which suggests a possible causal mechanism for how inequality and heterogeneity can emerge, persist, and increase in observed ecological and social–ecological systems.

### CRediT authorship contribution statement

**Natalie Davis:** Conceptualization, Formal analysis, Data curation, Methodology, Project administration, Resources, Software, Visualization, Writing – original draft, Writing – review & editing. **Andrew Jarvis:** Conceptualization, Funding acquisition, Supervision, Writing – review & editing. **J. Gareth Polhill:** Conceptualization, Funding acquisition, Methodology, Resources, Supervision, Writing – review & editing.

### Declaration of competing interest

The authors declare that they have no known competing financial interests or personal relationships that could have appeared to influence the work reported in this paper.

### Data availability

Links to code repository provided in manuscript

### Acknowledgements

Funding was provided by a joint Lancaster University/The James Hutton Institute, UK Ph.D. studentship to ND. The authors acknowledge useful comments from two anonymous reviewers, which helped sharpen the manuscript, and the efforts of the editor, Dr Michael Small, in finding said reviewers. In addition, ND acknowledges statistical advice from Dr Vicki Davis and discussions on the modelling framework with Dr Kirsti Ashworth, as well as feedback on model and experimental design from Dr Nanda Wijermans and Dr Émile Chappin at ESSA@work during Social Simulation Week 2020. The authors also acknowledge the Research/Scientific Computing teams at The James Hutton Institute and NIAB for providing computational resources and enduringly patient technical support for the “UK’s Crop Diversity Bioinformatics HPC” (BBSRC, UK grant BB/S019669/1) and the James Hutton Institute computing cluster, which were used to run the simulations reported within this paper. GP is grateful for funding from the Scottish Government’s Strategic Research Programme, UK 2022–27 (project JHI-C5-1).

### Appendix A. Supplementary data

Supplementary material related to this article can be found online at <https://doi.org/10.1016/j.physa.2022.128261>.

### References

- [1] A.J. Jarvis, S.J. Jarvis, C.N. Hewitt, Resource acquisition, distribution and end-use efficiencies and the growth of industrial society, *Earth Syst. Dyn.* 6 (2) (2015) 689–702, <http://dx.doi.org/10.5194/esd-6-689-2015>.
- [2] Y. Wang, et al., Global evidence of positive biodiversity effects on spatial ecosystem stability in natural grasslands, *Nature Commun.* 10 (1) (2019) 1–9, <http://dx.doi.org/10.1038/s41467-019-11191-z>.
- [3] J. Tews, et al., Animal species diversity driven by habitat heterogeneity/diversity: The importance of keystone structures, *J. Biogeogr.* 31 (1) (2004) 79–92, <http://dx.doi.org/10.1046/j.0305-0270.2003.00994.x>.
- [4] A. Stein, K. Gerstner, H. Kreft, Environmental heterogeneity as a universal driver of species richness across taxa, biomes and spatial scales, *Ecol. Lett.* 17 (7) (2014) 866–880, <http://dx.doi.org/10.1111/ele.12277>.
- [5] L. Laanisto, et al., Microfragmentation concept explains non-positive environmental heterogeneity–diversity relationships, *Oecologia* 171 (1) (2013) 217–226, <http://dx.doi.org/10.1007/s00442-012-2398-5>.
- [6] I. Seiferling, R. Proulx, C. Wirth, Disentangling the environmental–heterogeneity–species–diversity relationship along a gradient of human footprint, *Ecology* 95 (8) (2014) 2084–2095, <http://dx.doi.org/10.1890/13-1344.1>.
- [7] S.M. Mattison, et al., The evolution of inequality, *Evolut. Anthropol. Iss. News Rev.* 25 (4) (2016) 184–199, <http://dx.doi.org/10.1002/evan.21491>.
- [8] B.G. Charlton, The inequity of inequality, *J. Health Psychol.* 2 (3) (1997) 413–425, <http://dx.doi.org/10.1177/135910539700200309>.
- [9] J.E. Stiglitz, The price of inequality: How today’s divided society endangers our future, 2015, <http://dx.doi.org/10.7916/D8-96ED-6058>.
- [10] A. Gaye, *Access to Energy and Human Development*, no. 25, United Nations Development Programme, 2007, p. 21.
- [11] F. Perez-Escamilla, R.P. de Toledo Vianna, Food insecurity and the behavioral and intellectual development of children: A review of the evidence, *J. Appl. Res. Children* 3 (1) (2012) <https://eric.ed.gov/?id=EJ1189045> (Accessed: 19 Jan 2022).
- [12] B.K. Sovacool, The political economy of energy poverty: A review of key challenges, *Energy Sustain. Dev.* 16 (3) (2012) 272–282, <http://dx.doi.org/10.1016/j.esd.2012.05.006>.
- [13] M.A. Long, et al., Food insecurity in advanced capitalist nations: A review, *Sustainability* 12 (9) (2020) 3654, <http://dx.doi.org/10.3390/su12093654>.
- [14] C.M. Olson, Nutrition and health outcomes associated with food insecurity and Hunger, *J. Nutr.* 129 (2) (1999) 521, <http://dx.doi.org/10.1093/jn/129.2.521SS-524S>.
- [15] B.A. Laraia, Food insecurity and chronic disease, *Adv. Nutr.* 4 (2) (2013) 203–212, <http://dx.doi.org/10.3945/an.112.003277>.
- [16] S.N. Islam, *Inequality and Environmental Sustainability*, DESA Working Papers, (145) 2015, p. 30.



- [17] A. Dragulescu, V.M. Yakovenko, Statistical mechanics of money, *Eur. Phys. J. B - Condensed Matter Complex Syst.* 17 (4) (2000) 723–729, <http://dx.doi.org/10.1007/s100510070114>.
- [18] E.J.L. Chappin, G.P.J. Dijkema, Agent-based modelling of energy infrastructure transitions, *Int. J. Crit. Infrastruct.* 6 (2) (2010) 106–130, <http://dx.doi.org/10.1504/IJCIS.2010.031070>.
- [19] A. Fichera, A. Pluchino, R. Volpe, A multi-layer agent-based model for the analysis of energy distribution networks in urban areas, *Physica A* 508 (2018) 710–725, <http://dx.doi.org/10.1016/j.physa.2018.05.124>.
- [20] A.G. Dolfing, J.R.F.W. Leuven, B.J. Dermody, The effects of network topology, climate variability and shocks on the evolution and resilience of a food trade network, *PLoS ONE* 14 (3) (2019) 1–18, <http://dx.doi.org/10.1371/journal.pone.0213378>.
- [21] Y. Dou, et al., Land-use changes across distant places: design of a telecoupled agent-based model, *J. Land Use Sci.* 14 (3) (2019) 191–209, <http://dx.doi.org/10.1080/1747423X.2019.1687769>.
- [22] G. van Voorn, G. Hengeveld, J. Verhagen, An agent based model representation to assess resilience and efficiency of food supply chains, *PLoS ONE* 15 (2020) 1–27, <http://dx.doi.org/10.1371/journal.pone.0242323>.
- [23] G. ten Broeke, G. van Voorn, A. Ligtenberg, Which sensitivity analysis method should I use for my agent-based model? *J. Artif. Soc. Soc. Simul.* 19 (1) (2016) 1–35, <http://dx.doi.org/10.18564/jasss.2857>.
- [24] R.S. Beltran, J.W. Testa, J.M. Burns, An agent-based bioenergetics model for predicting impacts of environmental change on a top marine predator, the Weddell seal, *Ecol. Model.* 351 (2017) 36–50, <http://dx.doi.org/10.1016/j.ecolmodel.2017.02.002>.
- [25] Y. Liu, et al., A new multi-agent system to simulate the foraging behaviors of physarum, *Nat. Comput.* 16 (1) (2017) 15–29, <http://dx.doi.org/10.1007/s11047-015-9530-5>.
- [26] M.L. Miller, et al., Time to fly: A comparison of marginal value theorem approximations in an agent-based model of foraging waterfowl, *Ecol. Model.* 351 (2017) 77–86, <http://dx.doi.org/10.1016/j.ecolmodel.2017.02.013>.
- [27] J. Nauta, P. Simoons, Y. Khaluf, Group size and resource fractality drive multimodal search strategies: A quantitative analysis on group foraging, *Physica A* 590 (2022) 126702, <http://dx.doi.org/10.1016/j.physa.2021.126702>.
- [28] J.M. Epstein, R. Axtell, *Growing Artificial Societies: Social Science from the Bottom Up*, Brookings Institution Press Complex adaptive systems, Washington, D.C., 1996.
- [29] L.R. Little, A.D. McDonald, Simulations of agents in social networks harvesting a resource, *Ecol. Model.* 204 (3–4) (2007) 379–386, <http://dx.doi.org/10.1016/j.ecolmodel.2007.01.013>.
- [30] W. Barfuss, et al., Sustainable use of renewable resources in a stylized social-ecological network model under heterogeneous resource distribution, *Earth Syst. Dyn.* 8 (2) (2017) 255–264, <http://dx.doi.org/10.5194/esd-8-255-2017>.
- [31] T. Holstein, M. Wiedermann, J. Kurths, Optimization of coupling and global collapse in diffusively coupled socio-ecological resource exploitation networks, *New J. Phys.* 23 (3) (2021) 033027, <http://dx.doi.org/10.1088/1367-2630/abe0db>.
- [32] N. Davis, Network Development ABM, Zenodo, 2021, <http://dx.doi.org/10.5281/zenodo.4911977>.
- [33] B. Hannon, Sense of place: geographic discounting by people, animals and plants, *Ecol. Econom.* 10 (2) (1994) 157–174, [http://dx.doi.org/10.1016/0921-8009\(94\)90006-X](http://dx.doi.org/10.1016/0921-8009(94)90006-X).
- [34] A. Vanderveldt, L. Oliveira, L. Green, Delay discounting: Pigeon, rat, human-does it matter? *J. Exper. Psychol. Animal Learn. Cognition* 42 (2) (2016) 141–162, <http://dx.doi.org/10.1037/xan0000097>.
- [35] F.P. Ramsey, A mathematical theory of saving, *Econ. J.* 38 (152) (1928) 543–559.
- [36] I. Lorscheid, B.-O. Heine, M. Meyer, Opening the black box of simulations: increased transparency and effective communication through the systematic design of experiments, *Comput. Math. Organ. Theory* 18 (1) (2012) 22–62, <http://dx.doi.org/10.1007/s10588-011-9097-3>.
- [37] J.W. White, et al., Ecologists should not use statistical significance tests to interpret simulation model results, *Oikos* 123 (4) (2014) 385–388, <http://dx.doi.org/10.1111/j.1600-0706.2013.01073.x>.
- [38] R. Core Team, R: A language and environment for statistical computing, in: R Foundation for Statistical Computing, Vienna, Austria, 2019, <http://www.r-project.org>.
- [39] G. Csardi, T. Nepusz, The igraph software package for complex network research, *Interj. Complex Sy* (1695) (2006).
- [40] V.M.R. Muggeo, Estimating regression models with unknown break-points, *Stat. Med.* 22 (19) (2003) 3055–3071, <http://dx.doi.org/10.1002/sim.1545>.
- [41] V.M.R. Muggeo, Segmented: an R package to fit regression models with Broken-line relationships, in: (R News), 2008, <https://cran.r-project.org/doc/Rnews/>.
- [42] H. Wickham, *Ggplot2: Elegant Graphics for Data Analysis*, Springer-Verlag, New York, 2016, <http://ggplot2.org>.
- [43] Y. Sun, Y. Chen, On the mechanism of phase transitions in a minimal agent-based macroeconomic model, *Physica A* 506 (2018) 613–624, <http://dx.doi.org/10.1016/j.physa.2018.04.019>.
- [44] A.S. Klyubin, D. Polani, C.L. Nehaniv, Tracking information flow through the environment: Simple cases of stigmergy, in: *Proceedings of the Ninth International Conference on the Simulation and Synthesis of Living Systems, ALIFE 04, 2004*, pp. 563–568.
- [45] V. Lecheval, et al., From foraging trails to transport networks: how the quality-distance trade-off shapes network structure, *Proc. R. Soc. B: Biol. Sci.* 288 (1949) (2021) <http://dx.doi.org/10.1098/rspb.2021.0430>.